J. Marine. Sci. Appl. (2009) 8:196-203
DOI: 10.1007/s11804-009-8035-y

The research on the highly efficient calculation method of 3-D frequency-domain Green function

YAO Xiong-liang, SUN Shi-li*, WANG Shi-Ping and YANG Shu-tao

College of Shipbuilding Engineering, Harbin Engineering University, Harbin 150001, China

Abstract: The traditional calculation method of frequency-domain Green function mainly utilizes series or asymptotic expansion to carry out numerical approximation, however, this method requires very careful zoning, thus the computing process is complex with many cycles, which has greatly affected the computing efficiency. To improve the computing efficiency, this paper introduces Gaussian integral to the numerical calculation of the frequency-domain Green function and its partial derivatives. It then compares the calculation result with that in existing references. The comparison results demonstrate that, on the basis of its sufficient accuracy, the method has greatly simplified the computing process, reduced the zoning and improved the computing efficiency.

Keywords: frequency-domain Green function; numerical approximation; Gaussian integral
CLC number: O241 **Document code:** A **Article ID:** 1671-9433(2009)03-0196-08

1 Introduction

Numerical calculation of Green function and its partial derivatives play an important role in hydrodynamics. When boundary element method is adopted to solve problems about fluid structure interactions, a large amount of calculation of Green function and its partial derivatives is required. However, it is difficult to compute the function and to control the accuracy due to the oscillation and singularity of the integrand of Green function and the integral interval that is infinite. Therefore, efficient and accurate calculation of Green function and its partial derivative is of great significance.

So far, there have been many successful algorithms. MIT's Newman[1-4] had done excellent work on the problem, but his work still needs further improvement on the aspects such as the tightness of derivation, zoning of calculation zones, and the realization of calculation, etc. On the basis of Newman, Wang Rusen[5] conducted numerical approximation of the 3-D free surface frequency-domain Green function and the surplus function of its derivatives with double Chebyshev polynomials, which had reached 5D accuracy. The 5D accuracy means that the five effective digits after the radius point are sufficiently precise. This method has been very mature and can complete numerical calculation of the Green function and its partial derivative at any point within the coordinate plane. However, the computing process is complex, which requires extremely careful zoning, and more cycles, and has thus affected its computing speed. In addition, in some zones, the accuracy is not so fine. Therefore, in this paper, Gaussian integral is introduced to the numerical calculation of Green function based on Wang Rusen's work, which has greatly simplified the computing process, reduced the zoning and improved computing efficiency, and brought the accuracy of the numerical results to at least 6D.

Received date: 2008-06-20.
Foundation item: Supported by the National Natural Science Foundation of China under Grant No.50779007; the National Science Foundation for Young Scientists of China under Grant No.50809018; the Specialized Research Fund for the Doctoral Program of Higher Education of China under Grant No.20070217074; the Defence Advance Research Program of Science and Technology of Ship Industry under Grant No.07J1.1.6; Harbin Engineering University Foundation under Grant No.HEUFT07069.
***Corresponding author Email:** sunshili19831119@163.com

2 Mathematical processing

2.1 Primary processing of $F(x, y)$ and its partial derivatives

Numerical calculation of 3-D free surface frequency-domain Green function at infinite water depth is summarized as the following principal integral:

$$F(KR,-KZ)=2\int_0^\infty \frac{1}{\kappa-K}\mathrm{e}^{-kZ}J_0(\kappa R)\mathrm{d}\kappa \quad (Z\le 0, R\ge 0), \tag{1}$$

where $K=\omega^2/g$ is wave number, ω is frequency, g is the acceleration of gravity, J_0 is zero-order Bessel function of the first kind. Given $x=KR$, $R=\sqrt{(x-x_0)^2+(y-y_0)^2}$, R denotes the horizontal distance between the field point and the source point, $y=-KZ$, $Z=-(z+\zeta)$. Newman[1] has given the expression for the Eq.(1) as follows:

$$F(x,y)=2\int_0^{\infty}\frac{1}{\kappa-1}\mathrm{e}^{-\kappa y}J_0(\kappa x)\mathrm{d}\kappa=$$
$$-\pi\mathrm{e}^{-y}[H_0(x)+Y_0(x)]-$$
$$2\int_0^{y}\mathrm{e}^{t-y}(x^2+t^2)^{-1/2}\mathrm{d}t, \tag{2}$$

where H_0 is zero-order Struve function, Y_0 is zero-order Bessel function of the second kind. When x is small, power series expansion is needed to calculate it, and automatic judgment principles are adopted for series truncation; when x is large, its asymptotic expansion is needed[6]. In Eq.(2), the third item is definite integral, when x is large, the change of integrand is gentle, so Gaussian integral can be applied in the calculation. In order to enhance the accuracy of calculation, Gaussian integral formula with 16 points is used in the paper; when x is small, in Eq.(2), the change of the third item is dramatic, Gaussian integral cannot guarantee sufficient accuracy. In this paper, the power series expansion of e^t is conducted, however, if y is large, the power series expansion of e^t can be difficult to converge, in which situation it needs to expand J_0 function into power series.

In Eq.(2), the partial derivatives of x and y are denoted by

$$\frac{\partial F(x,y)}{\partial y}=\frac{-2}{\sqrt{x^2+y^2}}-F(x,y), \tag{3}$$

$$\frac{\partial F(x,y)}{\partial x}=2\int_0^{Y}\mathrm{e}^{t-y}\cdot\frac{x}{(x^2+t^2)^{3/2}}\mathrm{d}t+$$
$$\pi\mathrm{e}^{-Y}[Y_1(x)+H_1(x)-\frac{2}{\pi}]. \tag{4}$$

From Eq.(3), $F(x,y)$ is got and then $\partial F(x,y)/\partial y$ can be obtained, while $\partial F(x,y)/\partial x$ requires specific processing.

2.2 Zoning

Based on the scope of the application of different algorithms, coordinate plane is divided into three zones by $x=0.4$, $y=4$, namely zone *A*, zone *B*, zone *C*, as shown in Fig.1. The zoning boundary is not set fixed; reasonable boundaries can be got through trials. The basic rule is improving calculation efficiency to the greatest extent on the basis of guaranteeing the accuracy. And the boundary $x=0.4$, $y=4$ is almost reasonable for most structures.

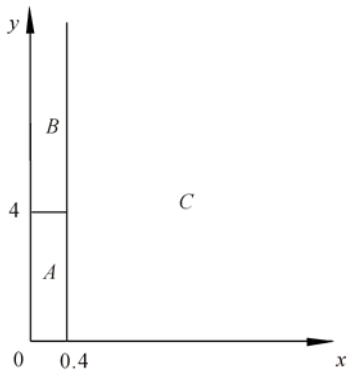

Fig.1 Zoning along coordinate plane

2.3 Numerical calculation of zone *A*

2.3.1 The approximate calculation formula of $F(x,y)$

Both x and y are small in zone *A*, where e^t in Eq.(2) is expanded to power series. Through continuous integration by parts, the following equations can be obtained:

$$F(x,y)=\mathrm{e}^{-y}\{-2J_0(x)\ln(y+\sqrt{x^2+y^2})-$$
$$[\pi Y_0(x)-2J_0(x)\ln x]-$$
$$\pi\sqrt{x^2+y^2}\frac{H_0(x)}{x}-$$
$$2\sqrt{x^2+y^2}\sum_{m=0}^{\infty}\sum_{n=1}^{\infty}C_{mn}x^{2m}y^n\}. \tag{5}$$

$$F(x,y)=\mathrm{e}^{-y}\{-2J_0(x)\ln(y+\sqrt{x^2+y^2})-$$
$$[\pi Y_0(x)-2J_0(x)\ln x]+R_1f_0(x^2,y)\}.$$
$$f_0(x^2,y)=-\pi H_0(x)/x-2\sum_{m=0}^{\infty}\sum_{n=1}^{\infty}C_{mn}x^{2m}y^n\ ,$$

where

$$C_{0n}=[(n+1)(n+1)!]^{-1},\qquad m>1;$$
$$C_{mn}=-(\frac{n+2}{n+1})C_{m-1,n+2},\qquad m>1.$$

When $x\to 0^+$, thus

$$\pi Y_0(x)-2J_0(x)\ln x\to -2\ln 2+2\gamma, \tag{6}$$

where γ=0.577, which is Euler's constant.

Substitute Eq.(6) into Eq.(5),

$$f_0(0,y)=2[-E_i(y)+\ln(y)+\gamma]/y.$$

2.3.2 Approximate calculation formula of $\partial F(x,y)/\partial x$

Calculate the partial derivative of x using $F(x,y)$'s expansion Eq.(5):

$$\frac{\partial F}{\partial x}=(-2\mathrm{e}^{-y})\{-J_1(x)\ln(y+\sqrt{x^2+y^2})+$$
$$[J_1(x)\ln x-\frac{\pi}{2}Y_1(x)-\frac{yJ_0(x)}{x\sqrt{x^2+y^2}}]+$$
$$[\frac{\sqrt{x^2+y^2}}{x}-\frac{\pi}{2}\frac{y^2H_0(x)}{x^2\sqrt{x^2+y^2}}]-\frac{\pi}{2}\frac{H_1(x)}{x}\sqrt{x^2+y^2}+$$
$$\frac{x}{\sqrt{x^2+y^2}}\sum_{m=0}^{\infty}\sum_{n=1}^{\infty}C_{mn}x^{2m}y^n+\frac{\sqrt{x^2+y^2}}{x}\sum_{m=1}^{\infty}\sum_{n=1}^{\infty}2mC_{mn}x^{2m}y^n\}. \tag{7}$$

where J_1, Y_1 and H_1 are respectively the 1st-order Bessel functions of the first kind and the second kind and the 1st-order Struve function. There are references[4] for their algorithm, in the end, the following Eq.(8) can be obtained

$$\frac{\partial F}{\partial x}=(-2\mathrm{e}^{-y})\{-J_1(x)\ln(y+R_1)+$$
$$\left[J_1(x)\ln x-\frac{\pi}{2}Y_1(x)-\frac{yJ_0(x)}{xR_1}\right]+ \tag{8}$$
$$\left[\frac{R_1}{x}-\frac{\pi}{2}\frac{y^2H_0(x)}{x^2R_1}\right]+\frac{x}{R_1}f_1(x^2,y)\}.$$

In Eq.(8), f_1 is denoted as the surplus function of $\partial F/\partial x$.

$$f_1(x^2,y)=-\frac{\pi}{2}H_1(x)\frac{R_1^2}{x^2}+\sum_{m=0}^{\infty}\sum_{n=1}^{\infty}C_{mn}x^{2m}y^n+$$
$$R_1^2\sum_{m=1}^{\infty}\sum_{n=1}^{\infty}2mC_{mn}x^{2m-2}y^n. \tag{9}$$

For the points on y axis, the following equation can be derived from above equation:

$$f_1(0,y)=\frac{\mathrm{e}^y}{2}+\frac{\mathrm{e}^y-1}{2y}+$$
$$\frac{1}{2y}\left[-E_1(y)+\ln y+r-1\right]-\left(1+\frac{y^2}{9}\right). \tag{10}$$

2.4 Numerical calculation method of zone *B*

2.4.1 The approximate calculation formula of $F(x,y)$

In zone *B*, e^t is expanded to Power Series, and its radius of convergence is related with the value of y. When x is small and y is large, expansion of e^t into power series does not guarantee the sufficient accuracy, in which situation $J_0(\kappa x)$ should be expanded to power series, which is then applied into the Eq.(2) for continuous integration by parts, then the following equation can be obtained:

$$F(x,y)=2\sum_{n=0}^{\infty}\frac{(-1)^n}{(n!)^2}\cdot(\frac{x}{2})^{2n}\int_0^{\infty}\frac{\kappa^{2n}}{\kappa-1}\mathrm{e}^{-ky}=$$
$$-2\mathrm{e}^{-y}E_i(y)+2\sum_{n=1}^{\infty}\frac{(-1)^n}{(n!)^2}\left(\frac{x}{2}\right)^{2n}\times \tag{11}$$
$$[\sum_{m=1}^{2n}\frac{(m-1)!}{y^m}-\mathrm{e}^{-y}E_i(y)].$$

2.4.2 Approximate calculation formula of $\partial F(x,y)/\partial x$

In Eq.(11), partial derivative of x:

$$\frac{\partial F}{\partial x}=-x\sum_{n=1}^{\infty}\frac{n}{(n!)^2}\cdot(-\frac{x^2}{4})^{n-1}\times$$
$$[\sum_{m=1}^{2n}\frac{(m-1)!}{y^m}-\mathrm{e}^{-y}E_i(y)]. \tag{12}$$

2.5 Numerical calculation method of zone *C*

Zone *C* is the largest zone among the three zones. Its numerical calculation can be carried out directly using Eq.(4) by Gaussian integral method. That's because the algorithms of H_0, H_1, Y_0 and Y_1 have been very mature. When x is small, power series form is adopted for their calculation; when x is large, their asymptotic expansion can be used. In zone *C*, the value of x is large, which means that the third item of Eq.(2) and the first item of Eq.(4) constitute a continuous function with gentle change, and therefore, in this paper, 16 Gauss points are adopted to calculate it to obtain at least 6D accuracy, with most zones reaching accuracy above 7D or 8D. Gaussian integral formula is as follows:

$$\int_{-1}^{1}f(x)\mathrm{d}x=\sum_{k=0}^{n}A_k\cdot f(x_k)+E_n. \tag{13}$$

In the Eq.(13), x_k is the coordinate of the kth Gauss point, A_k is the weighted factor, n is the total number of Gauss points, E_n is the error. Because the integral interval of Eq.(2) and Eq.(4) is [0, y], affine transformation is required to convert the integral interval into [-1,1], and then Eq.(13) can be directly applied.

3 Numerical results

3.1 Comparison between numerical results

Table 1 has presented the comparison between numerical results in this paper and that in Ref.[7], the numerical results in Ref.[7] can guarantee at least 5D accuracy.

The following conclusions can be reached.

1) Only when x is equal to 0.1 the points in Table1 are located in zone *A* and zone *B*, at this time, if y is smaller than or equivalent to 10, 6D accuracy can be achieved; and if y is equivalent to 20, accuracy is not so

good, but still can reach 5D. This is because the numerical results in zone B are related with the exponential integral $E_i(y)$. When y is small, in this paper, power series method is used to estimate it; when y is large, asymptotic expansion is used to estimate it; when y is equivalent to 20, the power series method is used for estimation of exponential integration. But the convergence radius of the exponential integral is related with the number of the series, namely, the higher the number, the greater the radius of convergence, the more accurate the results. If we expect more accurate results, the series number can be selected according to the corresponding value of y.

2) Zone C is Gaussian integral domain, most of its numerical results can achieve more than 7D accuracy, while only a few points have poorer accuracy, but it also guarantees 6D accuracy. This demonstrates that the introduction of Gaussian integral into numerical calculation of Green function is reasonable and effective.

Table 1 Comparison between numerical results

	x	0.1	0.1	0.1	0.1	0.1
	y	0.1	0.5	1	5	20
F	Ref.[6]	2.508 077 81	-0.579 258 39	-1.400 834 91	-0.541 378 79	-0.105 594 11
	This paper	2.508 077 69	-0.579 258 46	-1.400 834 95	-0.541 378 70	-0.105 591 50
	Error	1E-07	7E-08	4E-08	-9E-08	-3E-06
Fx	Ref.[6]	-6.821 542 27	-0.558 166 16	-0.129 127 58	0.003 075 98	0.000 029 78
	This paper	-6.821 542 27	-0.558 166 16	-0.129 127 58	0.003 075 98	0.000 029 65
	Error	0E+00	1E-09	-1E-09	2E-09	1E-07
Fy	Ref.[6]	-16.650 213 44	-3.343 064 31	-0.589 239 48	0.141 458 77	0.005 595 36
	This paper	-16.650 213 32	-3.343 064 23	-0.589 239 43	0.141 458 64	0.005 592 75
	Error	-1E-07	-8E-08	-5E-08	1E-07	3E-06
	x	0.5	0.5	0.5	0.5	0.5
	y	0.1	0.5	1	5	20
F	Ref.[6]	0.005 554 35	-1.109 086 84	-1.540 845 04	-0.537 697 05	-0.105 558 39
	This paper	0.005 554 31	-1.109 086 87	-1.540 845 06	-0.537 696 96	-0.105 558 39
	Error	4E-08	3E-08	2E-08	-9E-08	-4E-09
Fx	Ref.[6]	-5.098 066 92	-1.787 056 78	-0.526 880 98	0.015 300 8	0.000 148 74
	This paper	-5.098 066 94	-1.787 056 81	-0.526 880 99	0.015 300 8	0.000 148 73
	Error	2E-08	3E-08	2E-08	2E-08	3E-09
Fy	Ref.[6]	-3.927 877 05	-1.719 344 03	-0.248 009 34	0.139 682 17	0.005 589 63
	This paper	-3.927 877 01	-1.719 344 06	-0.248 009 32	0.139 682 05	0.005 589 62
	Error	-4E-08	-3E-08	-2E-08	1E-07	8E-09
	x	1	1	1	1	1
	y	0.1	0.5	1	5	20
F	Ref.[6]	-2.057 364 14	-2.005 492 94	-1.840 022 3	-0.526 319 33	-0.105 447 02
	This paper	-2.057 364 13	-2.005 492 94	-1.840 022 2	-0.526 319 25	-0.105 447 01
	Error	-1E-08	0E+00	-1E-08	-8E-08	-6E-09
Fx	Ref.[6]	-3.276 876 45	-1.629 511 79	-0.591 170 18	0.030 070 81	0.000 296 25
	This paper	-3.276 876 41	-1.629 511 76	-0.591 170 16	0.030 070 76	0.000 296 51
	Error	-4E-08	-3E-08	-1E-08	4E-08	-3E-07
Fy	Ref.[6]	0.067 289 76	0.216 638 56	0.425 808 73	0.134 087 06	0.005 571 78
	This paper	0.067 289 75	0.216 638 56	0.425 808 73	0.134 086 98	0.005 571 78
	Error	7E-09	4E-09	-4E-10	8E-08	4E-11

Continued table 1

	x	5	5	5	5	5
	y	0.1	0.5	1	5	20
F	Ref.[6]	1.365 442 14	0.783 703 65	0.319 848 05	-0.298 608 42	-0.102 062 54
	This paper	1.365 442 19	0.783 703 68	0.319 848 08	-0.298 608 42	-0.102 062 54
	Error	-5E-08	-3E-08	-3E-08	-4E-09	2E-09
Fx	Ref.[6]	0.914 567 84	0.639 252 66	0.418 081 88	0.044 982 58	0.001 341 84
	This paper	0.914 567 85	0.639 252 67	0.418 081 89	0.044 982 58	0.001 341 84
	Error	-8E-09	-1E-08	-6E-09	1E-09	-1E-09
Fy	Ref.[6]	-1.765 362 16	-1.181 718 52	-0.712 080 32	0.015 765 7	0.005 048 29
	This paper	-1.76 536 222	-1.181 718 56	-0.712 080 35	0.015 765 7	0.005 048 29
	Error	5E-08	4E-08	3E-08	-4E-09	-2E-09
	x	10	10	10	10	10
	y	0.1	0.5	1	5	20
F	Ref.[6]	-0.514 829 2	-0.410 999 65	-0.327 737 17	-0.187 468 41	-0.093 293 46
	This paper	-0.514 829 2	-0.410 999 63	-0.327 737 16	-0.187 468 41	-0.093 293 46
	Error	-2E-08	-2E-08	-1E-08	2E-09	-3E-09
Fx	Ref.[6]	1.435 237 56	0.969 651 11	0.595 314 06	0.026 437 82	0.002 042 55
	This paper	1.435 237 50	0.968 651 07	0.595 314 03	0.026 437 82	0.002 042 55
	Error	6E-08	1E-03	3E-08	-1E-09	2E-09
Fy	Ref.[6]	0.314 839 20	0.211 249 18	0.128 729 73	0.008 582 97	0.003 850 74
	This paper	0.314 839 18	0.211 2491 7	0.128 729 72	0.008 582 97	0.003 850 74
	Error	2E-08	1E-08	1E-08	-3E-09	2E-09
	x	20	20	20	20	20
	y	0.1	0.5	1	5	20
F	Ref.[6]	-0.455 906 71	-0.338 566 82	-0.244 667 90	-0.100 600 90	-0.072 518 07
	This paper	-0.455 906 71	-0.338 566 81	-0.244 667 90	-0.100 600 90	-0.072 518 06
	Error	1E-09	-6E-09	-3E-09	0E+00	-7E-09
Fx	Ref.[6]	-0.936 009 59	-0.625 778 28	-0.377 590 89	-0.002 307 62	0.001 910 57
	This paper	-0.936 009 51	-0.625 778 23	-0.377 590 86	-0.002 307 62	0.001 910 57
	Error	-8E-08	-5E-08	-3E-08	2E-09	4E-09
Fy	Ref.[6]	0.355 907 96	0.238 598 05	0.144 792 66	0.003 586 65	0.001 807 39
	This paper	0.355 907 96	0.238 598 05	0.144 792 66	0.003 586 65	0.001 807 39
	Error	-8E-10	6E-10	-3E-09	2E-10	5E-09

Note: In this paper, the numerical results just take the first eight decimal places into account, however, in actual calculation of error, more decimal places of effective number are taken into account. The error in all the tables of this paper means the absolute error which is the result of the magnitude in Ref.[6] minus that in this paper.

3.2 The variation trend of $F(x,y)$ and its partial derivatives

From Fig.2 we can see that, the variation trend of wave-making part of $F(x,y)$, namely the frequency-domain Green function along the x direction of the wave (the propagation direction of the surface wave) generally meets the cyclical variation law with continued amplitude attenuation, which is attenuating continuously along the y direction (direction of the increase in water depth). And this is consistent with the actual physical phenomenon. In this regard, $\partial F(x,y)/\partial x$ and $\partial F(x,y)/\partial y$ have the same variation law with $F(x,y)$. At the same time, it can be seen from the three figures that, the origin of planar coordinate system is at the

singular point. For the floating body, solving singularity problem in a reasonable manner is essential; however, for submerged body, there is no such singular problem. This is because such singular point only exists at the intersection between free surface and the surface of the body. And there now exists many numerical methods deposing such singular problems, but most of them are not satisfactory. In this paper, the Green function is used to compute the added mass and damping coefficients by numerical integral method, which means the elements near free surface are thought to be linear. In fact, the Green function near free surface is far from linear. So, the approximation makes the added mass and damping coefficients not very precise, especially for the damping coefficients.

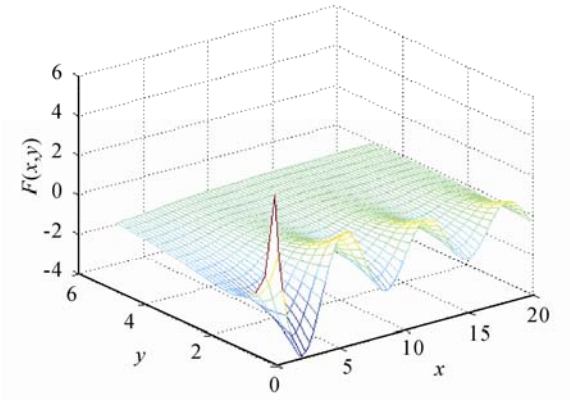

(a) The change of $F(x,y)$ along the coordinate plane

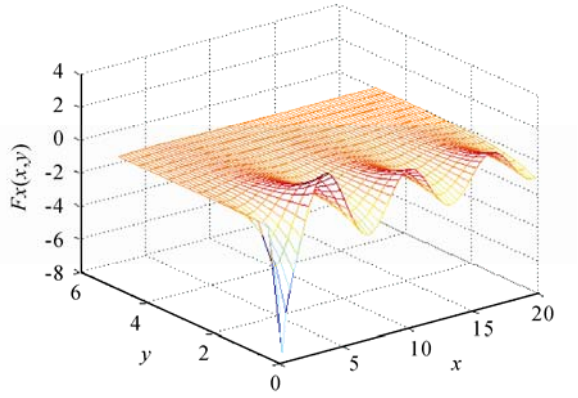

(b) The change of $\partial F(x,y)/\partial x$ along the coordinate plane

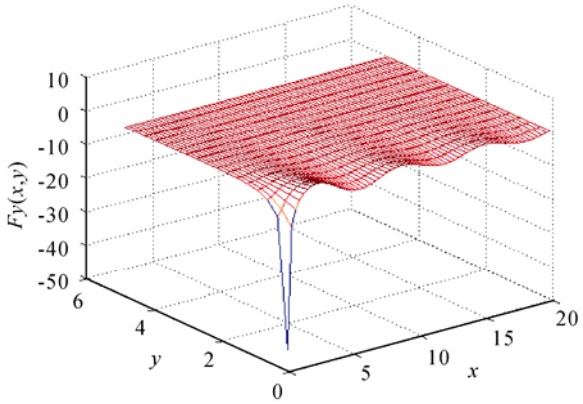

(c) The change of $\partial F(x,y)/\partial y$ along the coordinate plane

Fig.2 The change trend of $F(x,y)$ and its partial derivatives

3.3 The influence of Gauss points on accuracy

(2*n*+1)-order accuracy can be obtained adopting *n* Gauss points, and the accuracy is also related with the variation trend of integrand. This section discusses the influence of the amount of Gauss points on the calculation accuracy, so as to get some beneficial conclusions.

The calculation accuracy becomes worse along with augmentation of the value of *y* from Table 2. When the magnitude of y reaches 20, it can guarantees 5D accuracy using 8 Gauss points. This paper adopts 16 Gauss points to get more accuracy. If the dimension of actual underwater structure is smaller, the amount of Gauss points can be reduced. Therefore, appropriate Gauss points can be chosen according to the actual structure. While the change trend of calculation accuracy along with *x* is not listed in this paper. That's because the lager the magnitude of *x*, the higher the calculation accuracy. If it satisfies some accuracy when the value of *x* is chosen as 0.5, it must meet the accuracy when *x* is larger adopting the same Gauss points.

Table2 The influence of the amount of Gauss points on calculation accuracy

$x=0.5; y=0.1$	F	Fx	Fy
reference	0.005 554 35	-5.098 066 92	-3.927 877 05
2 Gauss points	0.005 555 46	-5.098 078 57	-3.927 878 16
Error	1E-006	-1E-005	-1E-006
4 Gauss points	0.005 554 31	-5.098 066 95	-3.927 877 01
Error	-4E-008	-3E-008	3E-008
6 Gauss points	0.005 554 31	-5.098 066 95	-3.927 877 01
Error	-4E-008	-3E-008	3E-008
$x=0.5; y=1$	F	Fx	Fy
reference	-1.540 845 04	-0.526 880 98	-0.248 009 34
2 Gauss points	-1.548 095 58	-0.458 407 54	-0.240 758 80
Error	-7E-003	-1E-001	-7E-003
4 Gauss points	-1.540 798 02	-0.528 026 36	-0.248 056 36
Error	4E-005	-1E-003	-4E-005
6 Gauss points	-1.540 845 08	-0.526 868 46	-0.248 009 31
Error	-3E-008	-1E-005	3E008
8 Gauss points	-1.540 845 07	-0.526 881 04	-0.248 009 32
Error	-1E-008	-6E-008	2E-008
$x=0.5; y=10$	F	Fx	Fy
reference	-0.225 901 73	0.001 564 99	0.026 151 26
2 Gauss points	-0.154 628 76	0.001 114 50	0.045 121 71
Error	7E-002	-4E-004	-2E-002
4 Gauss points	-0.224 970 26	0.001 536 93	0.025 219 79
Error	9E-004	-2E-005	-9E-004
6 Gauss points	-0.225 903 30	0.001 587 19	0.026 152 83
Error	-1E-006	2E-005	1E-006
8 Gauss points	-0.225 901 79	0.001 571 33	0.026 151 32
Error	-5E-008	6E-006	-5E-008
$x=0.5; y=20$	F	Fx	Fy
reference	-0.105 558 39	0.000 148 74	0.005 589 63
2 Gauss points	-0.018 507 80	0.000 037 16	-0.081 460 96
Error	8E-002	-1E-004	8E-002
4 Gauss points	-0.094 525 97	0.000 138 14	-0.005 442 79
Error	1E-002	-1E-005	-1E-002
6 Gauss points	-0.105 2643 8	0.000 148 52	0.005 295 62
Error	2E-004	-2E-007	2E-004
8 Gauss points	-0.105 555 74	0.000 148 74	0.005 586 98
Error	-2E-006	-3E-009	-2E-006

Accurate and fast calculation of Green function and its partial derivatives is the key to solve the problem of fluid structure interaction. This paper discusses the fast algorithm for 3-D frequency-domain Green function at infinite depth and its derivatives, and introduces Gaussian integral into the numerical calculation of the Green function and its partial derivatives. Numerical results show that the method can not only simplify the computing process, reduce the districts and improve computing efficiency, but also guarantees enough accuracy of the results. Therefore, this paper provides an effective method for the fast calculation of the Green function and its partial derivatives.

References

[1] NEWMAN J N. Double-accuracy evaluation of the report oscillatory source potential[J]. Journal of Ship Research, 1984, 28: 151-154.

[2] NEWMAN J N. An expansion of the oscillatory potential[J]. Applied Ocean Research, 1984, 6: 116-117.

[3] NEWMAN J N. Algorithms for the free-surface Green function[J]. Journal of Engineering Mathematics, 1985, 19: 57-67.

[4] ABRAMOWITZ M, STEGUN I A. Handbook of mathematical functions with formulas, Graphs and mathematical tables[M]. New York: Government Printing Office, 1964: 525-536.

[5] WANG Rusen. Numerical approximation of three-dimensional free-surface Green function and its partial derivatives (frequency-domain infinite water depth)[J]. Chinese Journal of Hydrodynamics, 1992, 7(3): 65-79(in Chinese).
[6] ZHOU Qingbiao, ZHANG Gang, ZHU Linsheng. Fast algorithm of Green function and its partial derivatives of free surface wave[J]. Chinese Journal of Computational Physics, 1999, 16(2): 145-152(in Chinese).
[7] YAO Xiongliang, ZHANG Aman, LIU Yuchen. Interaction of two three-dimensional explosion bubbles. Journal of Marine Science and Application, 2007, 6(2): 12-18(in Chinese).

YAO Xiong-liang professor, was born in 1963. He received his master degree and PhD in 1989 and 1992 from Harbin Engineering University respectively. Now he is a professor and the Dean of Shipbuilding Department, Harbin Engineering University, China. He is the author or co-author of many papers in national and international journals and conference proceedings. His research interest includes shipbuilding, vibration control, flow induced vibration, structural analysis of ships and many others. He has won many awards at national level.

三维频域格林函数的高效率计算方法研究

姚熊亮，孙士丽，王诗平，杨树涛

（哈尔滨工程大学 船舶工程学院，黑龙江 哈尔滨 150001）

摘　要：传统的频域格林函数计算方法主要采用级数或渐进展开式对其进行数值逼近，但这种方法需要非常细致的分区，计算过程复杂，循环次数也较多，极大地影响计算效率.将高斯积分引入到频域格林函数及其导数的数值计算，并将其计算结果与已有参考文献进行对比，证明该方法在满足足够精度的基础上，使计算过程大大简化，减少了分区，提高了计算效率.

关键词：频域格林函数；数值逼近；高斯积分法